BMJ Open Ophthalmology

Assessing photoreceptor structure in patients with traumatic head injury

Matthew E Braza,[1] Jonathon Young,[2] Thomas A Hammeke,[3] Scott E Robison,[1] Dennis P Han,[1] Clinton C Warren,[1] Joseph Carroll,[1,2,4] Kimberly E Stepien[5]

[1]Department of Ophthalmology & Visual Sciences, Medical College of Wisconsin, Milwaukee, Wisconsin, USA
[2]Department of Cell Biology, Neurobiology and Anatomy, Medical College of Wisconsin, Milwaukee, Wisconsin, USA
[3]Department of Psychiatry and Behavioral Medicine, Medical College of Wisconsin, Milwaukee, Wisconsin, USA
[4]Department of Biophysics, Medical College of Wisconsin, Milwaukee, Wisconsin, USA
[5]Department of Ophthalmology and Visual Sciences, University of WI – Madison, Madison, Wisconsin, USA

Correspondence to
Dr Kimberly E Stepien;
kstepien@wisc.edu

ABSTRACT

Objective Previous work using adaptive optics scanning light ophthalmoscopy (AOSLO) imaging has shown photoreceptor disruption to be a common finding in head and ocular trauma patients. Here an expanded trauma population was examined using a novel imaging technique, split-detector AOSLO, to assess remnant cone structure in areas with significant disruption on confocal AOSLO imaging and to follow photoreceptor changes longitudinally.

Methods and Analysis Eight eyes from seven subjects with head and/or ocular trauma underwent imaging with spectral domain optical coherence tomography, confocal AOSLO and split-detector AOSLO to assess foveal and parafoveal photoreceptor structure.

Results Confocal AOSLO imaging revealed hyporeflective foveal regions in two of eight eyes. Split-detector imaging within the hyporeflective confocal areas showed both remnant and absent inner-segment structure. Both of these eyes were imaged longitudinally and showed variation of the photoreceptor mosaic over time. Four other eyes demonstrated subclinical regions of abnormal waveguiding photoreceptors on multimodal AOSLO imagery but were otherwise normal. Two eyes demonstrated normal foveal cone packing without disruption.

Conclusion Multimodal imaging can detect subtle photoreceptor abnormalities not necessarily detected by conventional clinical imaging. The addition of split-detector AOSLO revealed the variable condition of inner segments within confocal photoreceptor disruption, confirming the usefulness of dual-modality AOSLO imaging in assessing photoreceptor structure and integrity. Longitudinal imaging demonstrated the dynamic nature of the photoreceptor mosaic after trauma. Multimodal imaging with dual-modality AOSLO improves understanding of visual symptoms and photoreceptor structure changes in patients with head and ocular trauma.

Key messages

What is already known about this subject?
► Previous work using adaptive optics scanning light ophthalmoscopy (AOSLO) imaging has shown photoreceptor disruption to be a common finding in head and ocular trauma patients.

What are the new findings?
► This study uses multimodal AOSLO imaging both to further examine cellular photoreceptor disruption secondary to trauma and to follow these changes longitudinally, demonstrating the dynamic nature of the photoreceptor mosaic over time in response to trauma.

How might these results change the focus of research or clinical practice?
► The ability of multimodal AOSLO to resolve intact as well as absent inner-segment photoreceptors serves a valuable role in better understanding of the effects of head and ocular trauma on the photoreceptor mosaic and vision.

INTRODUCTION

One common ocular manifestation following trauma is commotio retinae (CR), a transient opacification of the retina thought to result from photoreceptor disruption.[1–3] Visual sequelae of CR range from transient blurred to permanent loss of vision, with many reports demonstrating spontaneous improvement in vision over time.[4–7] CR has been well studied with optical coherence tomography (OCT). Common OCT findings include an increase in reflectivity/intensity of the hyper-reflective band attributed to the inner-segment/outer-segment junction,[4 6 8–10] also called the ellipsoid zone (EZ); however, loss or attenuation of this band has also been noted.[5 7 10] Recovery of the EZ has been reported,[4 7 8 10] as has persistent disruption.[5 6 9 10] Given the range of OCT findings in CR, grading systems have been proposed to better predict functional recovery, which suggest that recovery of vision is dependent on the region and extent of the initial photoreceptor disruption, with the integrity of the EZ important for visual recovery.[11 12]

While assessing photoreceptor integrity is possible with OCT, the limited lateral resolution of OCT precludes visualisation of individual photoreceptors. By correcting for the eye's monochromatic aberrations, adaptive optics scanning light ophthalmoscopy (AOSLO) provides in vivo imaging of the photoreceptor mosaic with cellular resolution,[13 14] potentially holding prognostic value for patients suffering from head trauma. In an increasing number of cases, AOSLO has

revealed subclinical photoreceptor abnormalities that have evaded detection with clinical examination and/or OCT, suggesting that photoreceptor disruption may exist even with a normal-appearing OCT.[15]

AOSLO previously used to investigate outer-segment structure abnormalities following head and/or closed globe blunt ocular trauma has demonstrated persistent and variable manifestations of photoreceptor mosaic disruption in all patients studied.[15–17] However, it is unknown if these photoreceptor disruptions change with time and if remnant photoreceptor structure remains in areas of the mosaic where significant disruption and variable waveguiding exist on confocal AOSLO. Recently a novel imaging technique, non-confocal, split-detector AOSLO, was developed which allows for visualisation of photoreceptor inner-segment structure independent of the photoreceptor's ability to waveguide light.[18] To better understand the pathogenesis of their visual sequelae, we imaged patients with visual complaints following head and/or ocular trauma, with several of these patients followed longitudinally. By using both confocal and non-confocal, split-detector AOSLO, we sought to better characterise macular inner-segment photoreceptor structure in these patients and to begin exploring the relationship between retained photoreceptor structure and visual prognosis.

METHODS
Human subjects
Informed consent was obtained from all subjects prior to imaging. Axial length was measured in all eyes (IOL Master, Carl Zeiss Meditec, Dublin, California) to allow for accurate lateral scaling of retinal images. Prior to retinal imaging, eyes were dilated and accommodation suspended with one drop each of phenylephrine hydrochloride (2.5%) and tropicamide (1%).

Eight eyes from seven patients (five male; two female) with trauma-related visual complaints were recruited (online supplementary table 1). Three of seven patients were clinically diagnosed with CR, while the remaining patients were recruited due to known head trauma. Age (range=17–47 years, mean=27.4 years), cause of trauma, chief complaint leading the subject to seek ophthalmological care, time from trauma to imaging (range=14 days–10 years, mean=43 months) and visual acuity varied between subjects. Two subjects, WW_0923 and KS_0552, had been imaged previously and were reimaged in this study for longitudinal evaluation.[15 16 19]

Spectral domain OCT
Spectral domain OCT (SD-OCT) images (Bioptigen, Durham, North Carolina, USA) were obtained prior to AOSLO imaging for all individuals. High-resolution 4 mm line scans (1000 A-scans/B-scan; 120 repeated B-scans) were acquired horizontally and vertically through the fovea. These scans were registered and averaged to reduce speckle noise. Additionally, volumetric scans of the macula of either 3×3 mm (400 A-scans/B-scan; 400 B-scans/volume) and/or 7×7 mm (1000 A-scans/B-scan; 250 B-scans/volume) in size were acquired and were used to generate en-face OCT images from custom software.[19]

Adaptive optics scanning light ophthalmoscopy
Simultaneous confocal and split-detector AOSLO images of the macular photoreceptor mosaic were obtained using previously described technique, allowing for exact spatial registration.[14 18] A 790 nm superluminescent diode was used for retinal imaging sequences. Locations of the central fovea were sampled by instructing the patient to fixate at specific locations of the scanning raster. The parafoveal photoreceptor mosaic was also imaged horizontally and vertically in a strip-like manner extending out to 10° temporal and 5° superior, nasal and inferior by having the patient fixate on an adjustable fixation target. Image sequences containing 150–175 frames at each individual location were registered and processed according to a previously described strip registration algorithm (Python; Python Software Foundation).[20] Final images from each respective image sequence were montaged and manually blended using commercial software (Adobe Photoshop; Adobe Systems, San Jose, California). In subjects that were imaged longitudinally, photoreceptor lesions were location-matched by using reliable retinal landmarks such as blood vessels, ensuring analysis of the same foveal regions over time. Regions in near proximity were further aligned and dewarped with publicly available imaging software (FIJI plug-in bUnwarpJ; ImageJ). For one subject, longitudinal cone density measurements of the same foveal regions were taken using a custom semiautomated cone counting program that identified cones based on analysis of local intensity maxima over a 55 µm sampling window.[21] Images were viewed in both linear and logarithmic scales to assist in identifying dimly reflecting cones, while non-waveguiding 'dark' cones were not counted. The counts were then manually adjusted by a single observer (JY), and final density outputs were reported.[21]

RESULTS
SD-OCT imaging
Macular SD-OCT line scans of four eyes revealed no outer retinal abnormalities, while two eyes (CW_10303 and TH_10619) demonstrated subtle focal irregularities at the level of the interdigitation zone (IZ) and EZ bands, but without disruption (figure 1). The other two eyes displayed clinically apparent outer retinal disruption with loss of structure on SD-OCT, ranging from a focal outer lamellar defect through the IZ and EZ bands (figure 2A, WW_0923) to diffuse IZ disruption through the macula (figure 3A, KS_0552).

Confocal AOSLO imaging
Confocal AOSLO imaging of all eyes demonstrated variable findings. Of the six eyes with intact outer retinal structure on SD-OCT, contiguous, intact photoreceptor mosaics were visualised in the central fovea and extending
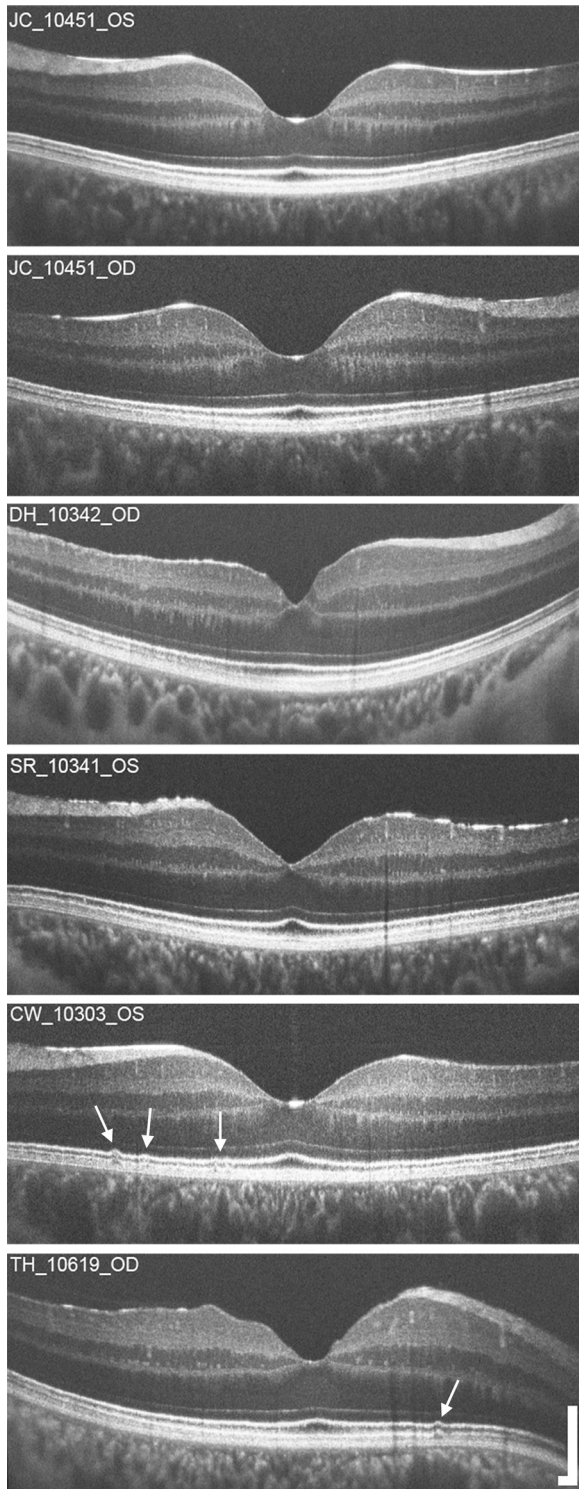
Figure 1 Macular horizontal spectral domain optical coherence tomography line scans through the fovea in patients with head and/or ocular trauma. No outer retinal abnormalities were observed in subjects JC_10451, SR_10341 and DH_10342. Subtle focal interdigitation zone and ellipsoid zone band irregularities (white arrows) were present in CW_10303 and TH_10619. Scale bar=200 µm.

10° temporally and 5° superiorly, inferiorly and nasally on confocal AOSLO. Foveal mosaics for four subjects are shown in figure 4.

However, confocal AOSLO did reveal focal circular hyper-reflective regions of 25–40 µm in size in four of the six eyes (CW_10303, SR_10341, JC_10451 OU). Confocal and split-detector images of these regions are shown in figure 4A–F$_{split}$. These regions are characteristically hyper-reflective on confocal and appear like small mounds on split-detector. No SD-OCT EZ or IZ band irregularities were observed in these regions.

Two eyes (WW_0923 and KS_0552) demonstrated well-defined regions of non-waveguiding, foveal photoreceptor mosaic disruption that appear black on confocal AOSLO imaging (figure 2B, WW_0923 and figure 3B, KS_0552).

Split-detector AOSLO imaging

In subjects WW_0923 and KS_0552, split-detector AOSLO was used to assess inner-segment photoreceptor integrity in areas of photoreceptor mosaic disruption that were non-waveguiding on confocal AOSLO. Split-detector AOSLO revealed several areas where inner-segment photoreceptor structure still remained (figures 2C,F and 5B,B3, white arrows), indicating likely outer-segment irregularities in this area and/or alteration of the alignment of these photoreceptors that prevent them from waveguiding light. Split-detector AOSLO also showed areas without inner-segment structure present (figures 2C,F and 5B1, black arrows), revealing true loss of photoreceptor structure as a result of the ocular trauma.

Longitudinal imaging

Subjects WW_0923 and KS_0552 both underwent further imaging approximately 30 months after initial imaging sessions. Subject WW_0923 is a 24-year-old man who sustained ocular trauma as a result of being an unrestrained driver in a motor vehicle collision in which airbags were deployed. Initial imaging at 7 and 22 months after trauma has been previously described.[16 19] Clinically, he complained of a persistent central scotoma with visual acuity stable at 20/25 at his most recent imaging session, 52 months post-trauma (figure 2D–F).

When compared with imaging 22 months post-trauma (figure 2A–C), outer retinal structure at 52 months post-trauma shows less disruption (figure 2D–F). Longitudinal SD-OCT imaging illustrates improvement of the outer lamellar defect with closure of breaks in the EZ and IZ bands. FocalRetina pigment epithelium irregularities as well as a tuft of debris seen in the foveal pit persist (figure 2A,D). The initial large triangular-shaped area of non-waveguiding photoreceptors on confocal AOSLO imaging is significantly smaller on subsequent imaging (figure 2B, initial; figure 2E, 30 months later). Split-detector AOSLO imaging at 52 months post-trauma revealed a near contiguous mosaic of photoreceptors, including an improved bottom right region (figure 2F), suggesting inner-segment recovery from prior imaging (figure 2C).
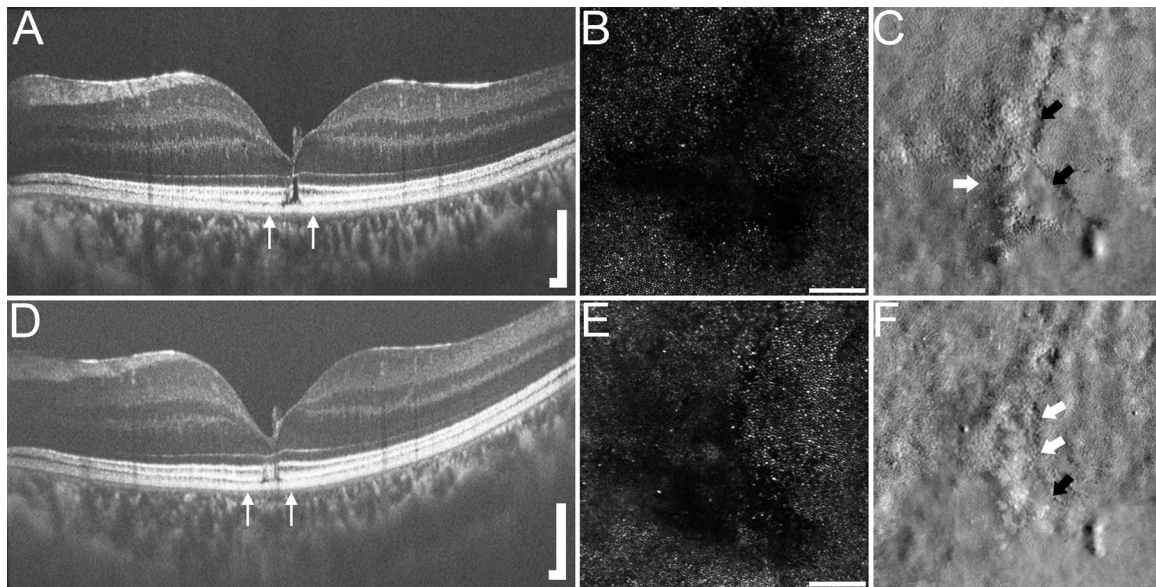
Figure 2 Multimodal imaging of the left eye for subject WW_0923 at 22 months (A,B,C) and 52 months (D,E,F) after trauma. Macular horizontal SD-OCT line scan revealed a persistent, focal outer lamellar defect with EZ and IZ disruption (A), which improved over time (D). Thin white arrows in (A) and (D) indicate area of AOSLO imaging. Confocal macular AOSLO imaging demonstrated a large anchor-shaped area of non-waveguiding photoreceptors (B), which is smaller in size on follow-up (E). Split-detector AOSLO images of the same location revealed a similar anchor-shaped disruption with both regions of intact inner-segment photoreceptors (white arrow) and areas devoid of inner-segment structure (black arrows) (C). Split-detector AOSLO imaging at 52 months post-trauma (F) showed inner-segment photoreceptor structure in areas previously without structure (F, white arrows), although focal areas of absent inner-segment structure still exist (F, black arrow). A and D: scale bar=200 µm; B, C, E and F: scale bar=100 µm. AOSLO, adaptive optics scanning light ophthalmoscopy; EZ, ellipsoid zone; IZ, interdigitation zone; SD-OCT, spectral domain optical coherence tomography.
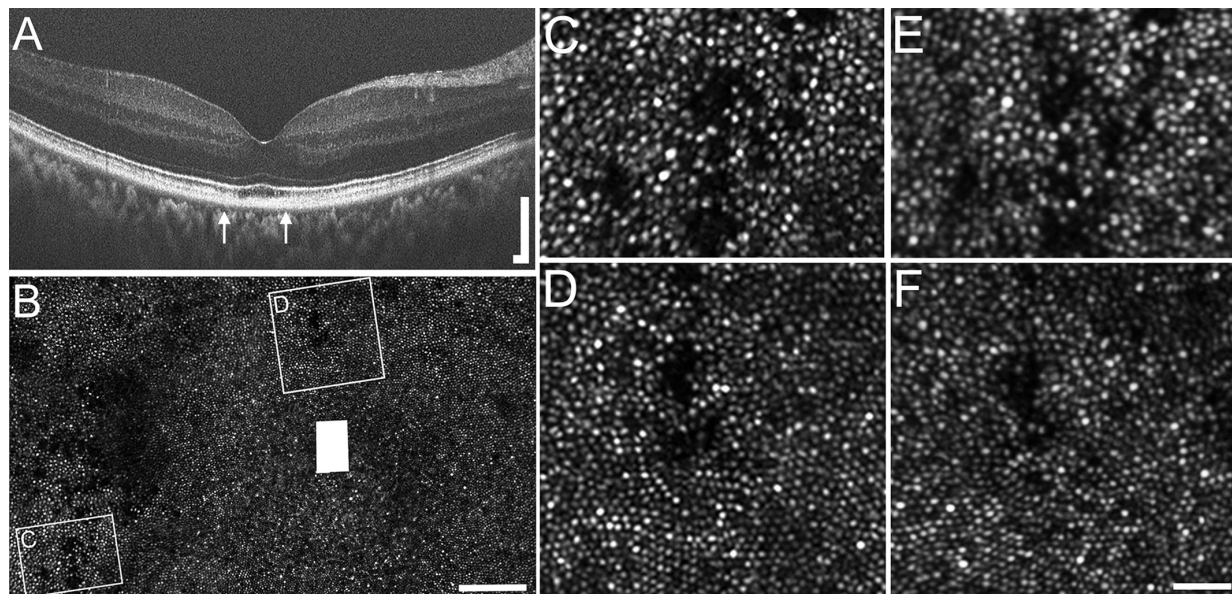

Figure 3 Multimodal imaging of the right eye for subject KS_0552 5 years post-trauma (A–D) and 8 years post-trauma (E,F). Macular horizontal SD-OCT line scan reveals focal foveal IZ disruption (A). Confocal AOSLO imaging of the foveal photoreceptor mosaic between the thin white arrows on (A) is shown in (B), which demonstrates multiple regions of dark, non-waveguiding photoreceptors. Two distinct regions of photoreceptor disruption (C,D) were chosen and compared with their identical regions on follow-up imaging performed 30 months after initial imaging (E,F), revealing similar structure and cone densities for both regions of interest. A: scale bar=200 µm; B: scale bar=100 µm; C–F: scale bar=25 µm. AOSLO, adaptive optics scanning light ophthalmoscopy; IZ, interdigitation zone; SD-OCT, spectral domain optical coherence tomography.
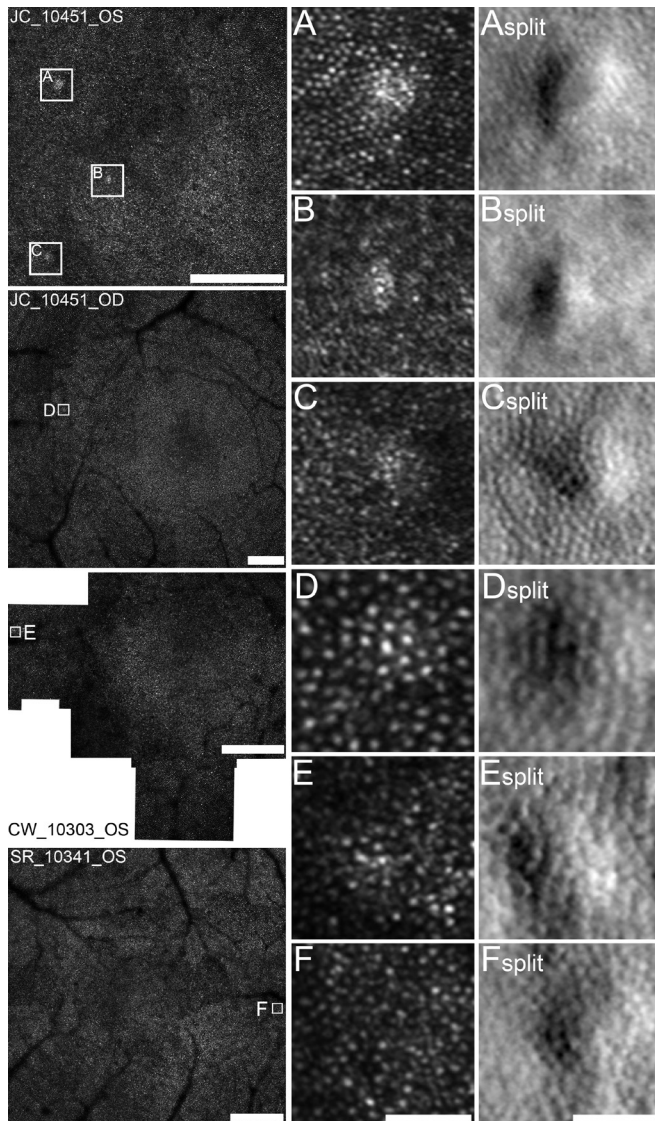
Figure 4 Confocal and split-detector AOSLO subclinical photoreceptor mosaic anomalies. Focal regions of abnormal waveguiding photoreceptors were found in confocal AOSLO foveal mosaics in subjects JC_10451 OD & OS, CW_10303 OS and SR_10341 OS (white boxes). Magnified views of these regions show focal hyper-reflective waveguiding cones with confocal AOSLO imaging (A–F) and focal mounding of photoreceptor inner-segment structure on split-detector AOSLO imaging (A$_{split}$–F$_{split}$), ranging from 25 µm to 40 µm in size. Montages: scale bar=300 µm. A–F$_{split}$: scale bar=40 µm. AOSLO, adaptive optics scanning light ophthalmoscopy.
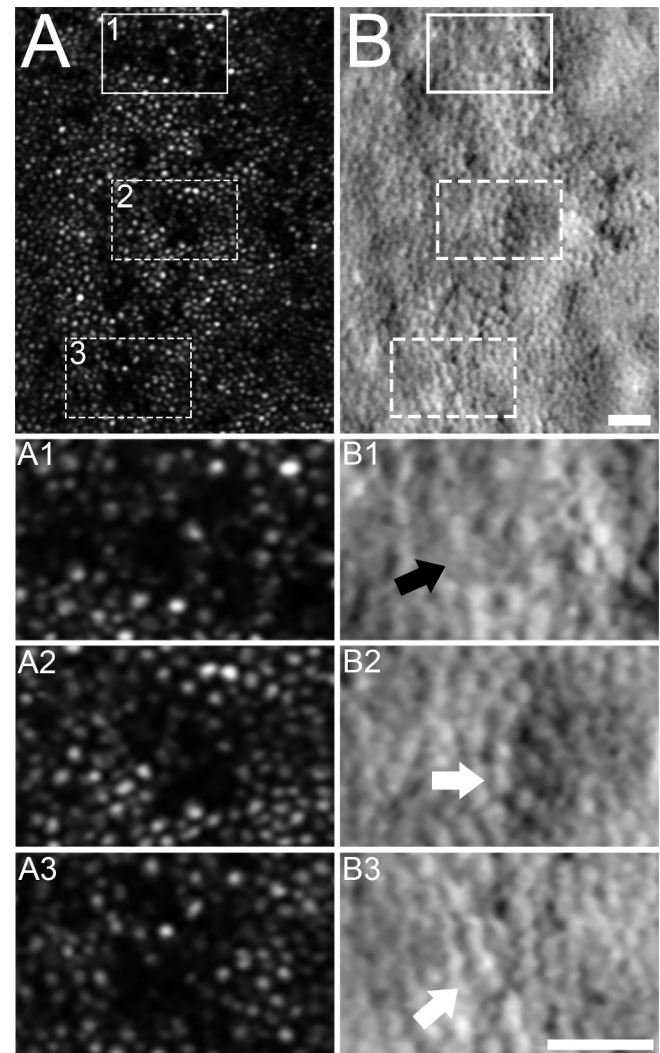

Figure 5 Confocal and split-detector AOSLO imaging in areas of photoreceptor mosaic disruption in subject KS_0552. Foveal confocal AOSLO revealed multiple areas of non-waveguiding cone photoreceptors (A). Three of these regions (A1–A3) were compared with aligned corresponding split-detector images (B1–B3). Areas of both absent inner-segment structure (B1, black arrow) and remnant inner-segment photoreceptor structure (B2, B3, white arrows) were present in these areas of non-waveguiding confocal images. A–B3: scale bar=25 µm. AOSLO, adaptive optics scanning light ophthalmoscopy.

Subject KS_0552 is a 46-year-old man who described a central purple-red scotoma in his right eye just nasal to fixation following severe head trauma in an industrial accident. Initial confocal AOSLO imaging which occurred 5 years post-trauma revealed multiple regions of photoreceptor disruption (figure 3B) which corresponded to functional changes on visual field testing and microperimetry, although no outer retinal abnormalities were present on clinical SD-OCT at the time of presentation.[15] Subsequent imaging was acquired approximately 30 months after initial AOSLO imaging and 8 years after his industrial accident. Clinically, the patient reported a persistent scotoma.

Two regions of photoreceptor disruption temporal and superior to the fovea were followed longitudinally by confocal AOSLO (figure 3C,D, initial; figure 3E,F, 30 months later). Areas of non-waveguiding photoreceptors appeared stable over this time period. Using a semiautomated cone identification program,[21] a 55 µm sampling window was used to compare cone densities in these two regions between two imaging sessions. The first region initially had a cone density of 40 498 cones/mm^2 on initial imaging (figure 3C) with 39 538 cones/mm^2 at follow-up (figure 3E), a difference of 960 cones/

mm^2. The second region had an initial cone density of 54 661 cones/mm^2 (figure 3D) compared with 52 796 cones/mm^2 on follow-up (figure 3F), a difference of 1865 cones/mm^2. Cone density measurements from both regions over time fall within the expected repeatability of confocal values for parafoveal cone density measurement,[21] indicating very stable structure between the two time points.

DISCUSSION

The extent of macular photoreceptor involvement following ocular and head trauma, what photoreceptor structure remains in areas with outer retinal involvement, and whether these disruptions in the photoreceptor mosaic are stable over time are not clear.[15–17] By using an expanded patient population, longitudinal imaging and multimodal imaging including both confocal and split-detector AOSLO, this case series begins to explore these questions.

The present study provides evidence that outer retinal disruption, both gross and subclinical, can occur in some patients following traumatic head injury.[15–17] While all patients in the current study presented with visual complaints following trauma, many of them had normal macular imaging findings (figures 1 and 4). This highlights the variability between functional vision changes perceived by the patient and retinal structural abnormalities that can be detected with multimodal imaging following head and ocular trauma. Some of this variability may be in part due to the degree and type of trauma and time to follow-up.

The AOSLO photoreceptor anomalies found in subjects CW_10303, SR_10341 and JC_10451 shown in figure 4A,F$_{split}$ illustrate that clinical imaging modalities alone may not provide clinicians with the complete picture of the extent of damage as a result of trauma. This highlights the utility of multimodal imaging in the detection of subtle photoreceptor abnormalities not necessarily detected by conventional clinical imaging. Prior studies have noted similar findings.[15 16]

Furthermore, multimodal AOSLO imaging can help to better delineate the anatomical disruptions at the level of the photoreceptor mosaic. Areas that appear dark with confocal AOSLO may represent areas with residual photoreceptor structure that cannot waveguide light or may be areas devoid of photoreceptor structure entirely. In subject WW_0923, a significant portion of the triangular foveal photoreceptor disruption visualised by confocal AOSLO still had residual inner-segment structure on split-detector AOSLO, suggesting this region may have a better possibility to recover function with time. Alternatively, areas lacking inner-segment structure as seen in the bottom right portion of this lesion have a much worse prognosis (figure 2C,F, black arrows). The ability of split-detector AOSLO to resolve intact as well as absent inner-segment photoreceptors serves a valuable role in determining the degree of residual cone structure

in these patients. This has been demonstrated in other retinal pathologies as well.[22 23]

AOSLO imaging has shown that dynamic changes can occur at the level of photoreceptor mosaic over time.[22] In this series, we demonstrated how AOSLO can confirm both change to the photoreceptor mosaic with time, as seen in subject WW_0923 (figure 2B,C,E,F), and stability of structure over time, as seen with subject KS_0552 (figures 3C–F , and 5). These structural findings evolve our knowledge that in the traumatic head injury population, the photoreceptor mosaic can be dynamic and change with time, consistent with prior clinical evidence that vision may spontaneously improve in CR after trauma.[4–7]

Limitations of this study include a small sample size, only two longitudinally followed eyes, variable time between trauma and research imaging, and lack of acute imaging immediately following trauma. While we were able to comment on two subjects longitudinally, conclusions regarding the relationship between retinal structure in initial presentation of subjects to their ophthalmologist and subsequent recovery cannot be made for other subjects. It would be of interest to image head trauma patients closer to their initial trauma with frequent longitudinal follow-up to better determine photoreceptor change in this population.

This case series confirms the usefulness of dual-modality AOSLO imaging in assessing photoreceptor structure and integrity in this population, which will help arm clinicians with an improved understanding of visual symptoms and prognosis for patients with ocular and/or head trauma. While dual-modality AOSLO provides unique structural insight in photoreceptor recovery following head trauma, we cannot say anything about the functional status of these cones. In the future, it will be important to assess these patients with tools such as adaptive optics-guided microperimetry which will allow for better correlation between visual function and cellular structure, providing clinicians with more information on visual prognosis in this population.[24]

Ethics approval This research project was approved by the Institutional Review Board at the Medical College of Wisconsin and followed the tenets of the Declaration of Helsinki.

Provenance and peer review Not commissioned; externally peer reviewed.

Open access This is an open access article distributed in accordance with the Creative Commons Attribution Non Commercial (CC BY-NC 4.0) license, which permits others to distribute, remix, adapt, build upon this work non-commercially, and license their derivative works on different terms, provided the original work is properly cited, appropriate credit is given, any changes made indicated, and the use is non-commercial. See: http://creativecommons.org/licenses/by-nc/4.0/

REFERENCES

1. Williams DF, Mieler WF, Williams GA. Posterior segment manifestations of ocular trauma. *Retina* 1990;10:S35–S44.
2. Sipperley JO, Quigley HA, Gass DM. Traumatic retinopathy in primates. The explanation of commotio retinae. *Arch Ophthalmol* 1978;96:2267–73.
3. Mansour AM, Green WR, Hogge C. Histopathology of commotio retinae. *Retina* 1992;12:24–8.
4. Itakura H, Kishi S. Restored photoreceptor outer segment in commotio retinae. *Ophthalmic Surg Lasers Imaging* 2011;42 Online:e29–31.
5. Ismail R, Tanner V, Williamson TH. Optical coherence tomography imaging of severe commotio retinae and associated macular hole. *Br J Ophthalmol* 2002;86:473a–4.
6. Sony P, Venkatesh P, Gadaginamath S, *et al*. Optical coherence tomography findings in commotio retina. *Clin Exp Ophthalmol* 2006;34:621–3.
7. Oladiwura D, Lim LT, Ah-Kee EY, *et al*. Macular optical coherence tomography findings following blunt ocular trauma. *Clin Ophthalmol* 2014;8:989–92.
8. El Matri L, Chebil A, Kort F, *et al*. Optical coherence tomographic findings in Berlin's Edema. *J Ophthalmic Vis Res* 2010;5:127–9.
9. Oh J, Jung JH, Moon SW, *et al*. Commotio retinae with spectral-domain optical coherence tomography. *Retina* 2011;31:2044–9.
10. Souza-Santos F, Lavinsky D, Moraes NS, *et al*. Spectral-domain optical coherence tomography in patients with commotio retinae. *Retina* 2012;32:711–8.
11. Ahn SJ, Woo SJ, Kim KE, *et al*. Optical coherence tomography morphologic grading of macular commotio retinae and its association with anatomic and visual outcomes. *Am J Ophthalmol* 2013;156:994–1001.
12. Chen H, Lu Y, Huang H, *et al*. Prediction of visual prognosis with spectral-domain optical coherence tomography in outer retinal atrophy secondary to closed globe trauma. *Retina* 2013;33:1258–62.
13. Rossi EA, Chung M, Dubra A, *et al*. Imaging retinal mosaics in the living eye. *Eye* 2011;25:301–8.
14. Dubra A, Sulai Y. Reflective afocal broadband adaptive optics scanning ophthalmoscope. *Biomed Opt Express* 2011;2:1757–68.
15. Stepien KE, Martinez WM, Dubis AM, *et al*. Subclinical photoreceptor disruption in response to severe head trauma. *Arch Ophthalmol* 2012;130:400–2.
16. Flatter JA, Cooper RF, Dubow MJ, *et al*. Outer retinal structure after closed-globe blunt ocular trauma. *Retina* 2014;34:2133–46.
17. Kaizu Y, Nakao S, Yamaguchi M, *et al*. Detection of airbag impact-induced cone photoreceptor damage by adaptive optics scanning laser ophthalmoscopy: a case report. *BMC Ophthalmol* 2016;16:99.
18. Scoles D, Sulai YN, Langlo CS, *et al*. In vivo imaging of human cone photoreceptor inner segments. *Invest Ophthalmol Vis Sci* 2014;55:4244–51.
19. Scoles D, Flatter JA, Cooper RF, *et al*. Assessing photoreceptor structure associated with ellipsoid zone disruptions visualized with optical coherence tomography. *Retina* 2016;36:91–103.
20. Dubra A, Harvey Z. Registration of 2D images from fast scanning ophthalmic instruments. In: Fischer B, Dawant B, Lorenz C, eds. *Biomedical Image Registration*. 1st edn. Berlin: Springer-Verlag, 2010: 60–71.
21. Garrioch R, Langlo C, Dubis AM, *et al*. Repeatability of in vivo parafoveal cone density and spacing measurements. *Optom Vis Sci* 2012;89:632–43.
22. Hansen S, Batson S, Weinlander KM, *et al*. Assessing photoreceptor structure after macular hole closure. *Retin Cases Brief Rep* 2015;9:15–20.
23. Scoles D, Sulai YN, Cooper RF, *et al*. Photoreceptor inner segment morphology in Best Vitelliform Macular Dystrophy. *Retina* 2017;37:741–8.
24. Wang Q, Tuten WS, Lujan BJ, *et al*. Adaptive optics microperimetry and OCT images show preserved function and recovery of cone visibility in macular telangiectasia type 2 retinal lesions. *Invest Ophthalmol Vis Sci* 2015;56:778–86.